SIAM J. APPL. MATH.
Vol. 46, No. 5, October 1986

SINGULAR HOPF BIFURCATION TO RELAXATION OSCILLATIONS*

S. M. BAER† AND T. ERNEUX‡

Abstract. Relaxation oscillations characterized by two quite different time scales are described by mathematical models of the form $x_t = f(x, y, \lambda, \varepsilon)$ and $y_t = \varepsilon g(x, y, \lambda, \varepsilon)$ where $\varepsilon \ll 1$ and λ is the control parameter. In this paper, we study the singular Hopf bifurcation from a basic steady state to these relaxation oscillations. Our bifurcation analysis shows how the harmonic oscillations near the bifurcation point progressively change to become pulsed, triangular oscillations.

In the second part of the paper, we present a numerical study of the FitzHugh–Nagumo equations for nerve conduction. We first observe that the numerical results are in good agreement with the analytical predictions. We then consider the switching from a stable steady state to a stable periodic solution, or the reverse transition. Our purpose is to explain the annihilation experiments described in the nerve conduction literature.

Key words. double zero eigenvalue, FitzHugh-Nagumo equations, chemical oscillations

1. Introduction. Relaxation oscillations characterized by two quite disparate time scales have been observed in many physical, chemical or biochemical systems. Many aspects of these oscillatory systems are accurately described by mathematical models of the form

$$x_t = f(x, y, \lambda, \varepsilon), \qquad y_t = \varepsilon g(x, y, \lambda, \varepsilon) \tag{1.1}$$

where x and y are two dependent variables (concentration of chemical intermediates, temperature, electrical current, etc.) and the subscript t denotes differentiation with respect to time t. The problem typically depends on two parameters: ε which is a small quantity and λ which is the control or bifurcation parameter. As λ is progressively increased, the solution of (1.1) suddenly changes from a steady state to large amplitude relaxation oscillations. The principal purpose of this paper is to analyze this transition.

To this end, we assume that (1.1) admits a basic steady-state solution given by

$$x = x_0(\lambda, \varepsilon), \qquad y = y_0(\lambda, \varepsilon) \tag{1.2}$$

which is stable (unstable) if

$$\lambda < \lambda_0(\varepsilon) \qquad (\lambda > \lambda_0(\varepsilon)). \tag{1.3}$$

If $\lambda = \lambda_0(\varepsilon)$ corresponds to a Hopf bifurcation point for time-period solutions [1], [2], then from the linearized theory, we have the following conditions for $\lambda_0(\varepsilon)$:

$$f_x(\lambda_0(\varepsilon), \varepsilon) + \varepsilon g_y(\lambda_0(\varepsilon), \varepsilon) = 0, \tag{1.4}$$

$$f_x(\lambda_0(\varepsilon), \varepsilon) g_y(\lambda_0(\varepsilon), \varepsilon) - f_y(\lambda_0(\varepsilon), \varepsilon) g_x(\lambda_0(\varepsilon), \varepsilon) > 0 \tag{1.5}$$

where f_x, f_y, g_x and g_y represent partial derivatives of f and g with respect to x or y and evaluated at $x = x_0$, $y = y_0$ and $\lambda = \lambda_0$. Examples of problems which satisfy these conditions are the models of mechanical or electronic oscillators of the van der Pol family [3] described by

$$y_{tt} + \Phi(y, \lambda, \varepsilon) y_t + \varepsilon y = 0 \tag{1.6}$$

* Received by the editors July 31, 1985.

† Mathematical Research Branch, NIADDK, National Institutes of Health, Bethesda, Maryland 20205.

‡ Department of Engineering Sciences and Applied Mathematics, Northwestern University, Evanston, Illinois 60201. The research of this author was supported by the Air Force Office of Scientific Research under grant AFOSR85-0150 and the National Science Foundation under grant DMS-8507922.

where $\Phi(y, \lambda, \varepsilon)$ is a nonlinear function of y. By defining $x \equiv \varepsilon^{-1} y_t$, (1.6) is equivalent to (1.1) with $f \equiv -\Phi(y, \lambda, \varepsilon)x - y$ and $g \equiv x$. Equation (1.1) with the assumptions (1.2)-(1.5) also describes many two-variable chemical or biochemical systems [4]-[9]. Then, the expressions for f and g may be more complicated. The recent interest in new chemical oscillators [10], [24], their mechanisms and possible applications in biology is the principal motivation of our bifurcation analysis.

Since $\lambda = \lambda_0$ corresponds to a Hopf bifurcation, time-periodic solutions of (1.1) can be constructed in the vicinity of $\lambda = \lambda_0$. We first define a small parameter η and a new time variable T by

$$\eta \equiv [(\lambda - \lambda_0(\varepsilon))/j]^{1/2}, \tag{1.7}$$

$$T \equiv \omega(\eta, \varepsilon)t = (\omega_0(\varepsilon) + \eta^2\omega_2(\varepsilon) \cdots)t, \tag{1.8}$$

where $j = \pm 1$ if $\lambda - \lambda_0(\varepsilon) \gtrless 0$ and $\omega(\eta, \varepsilon)$ is the unknown frequency of the oscillations. Then, we seek 2π-periodic solutions of (1.1) of the form

$$\begin{aligned} x(T, \varepsilon, \eta) - x_0(\lambda, \varepsilon) &= \eta x_1(T, \varepsilon) + \eta^2 x_2(T, \varepsilon) \cdots, \\ y(T, \varepsilon, \eta) - y_0(\lambda, \varepsilon) &= \eta y_1(T, \varepsilon) + \eta^2 y_2(T, \varepsilon) \cdots. \end{aligned} \tag{1.9}$$

We note that the coefficients appearing in the expansions (1.8) and (1.9) depend on ε. An analysis of simple problems reveal that the expansions (1.8) and (1.9) may become nonuniform as $\varepsilon \to 0$. Consider, for example, the following problem studied by Eckhaus [16]:

$$x_t = y - x^2 - x^3, \qquad y_t = -\varepsilon(x + \lambda). \tag{1.10}$$

The singular point $(x, y) = (x_0, y_0)$ where $x_0 = -\lambda$ and $y_0 = x_0^2 + x_0^3$, is unstable if $0 < \lambda < \frac{2}{3}$. In the vicinity of the bifurcation point $\lambda = \lambda_0 = 0$, the periodic solutions are given by

$$\begin{aligned} x - x_0 &= \eta 2\alpha \cos T - \eta^2 \varepsilon^{-1/2} \frac{4\alpha^2}{3} \sin 2T + O(\eta^3), \\ y - y_0 &= -\eta \varepsilon^{1/2} 2\alpha \sin T + \eta^2 2\alpha^2 (1 - \tfrac{1}{3} \cos 2T) + O(\eta^3) \end{aligned} \tag{1.11}$$

where $\eta = (\lambda - \lambda_0)^{1/2}$, $\alpha = (\frac{2}{3})^{1/2}$ and

$$T \equiv \omega t = \varepsilon^{1/2} \left(1 - \eta^2 \varepsilon^{-1} \frac{2\alpha^2}{3} + O(\eta^4)\right) t. \tag{1.12}$$

From either expression (1.11) for the periodic solution or the expansion for the frequency ω given in (1.12), we note that as $\varepsilon \to 0$, a singularity appears when

$$\varepsilon = O(\eta^2) \quad \text{or} \quad \varepsilon = O(|\lambda - \lambda_0|). \tag{1.13}$$

In addition, the analysis of (1.11) and (1.12) indicates that in this critical regime

$$x - x_0 = O(\varepsilon^{1/2}), \qquad y - y_0 = O(\varepsilon) \tag{1.14}$$

and

$$\omega = O(\varepsilon^{1/2}). \tag{1.15}$$

Similar conclusions have been obtained for different problems such as the FitzHugh-Nagumo (FHN) equations for nerve conduction [11], [12] (eqs. (3.8)).

In § 2, we investigate the singular Hopf bifurcation corresponding to (1.13)-(1.15). Since we are motivated by problems modeling chemical oscillations, we present in § 3 two applications of our theory. Section 4 is devoted to a numerical study of the FHN

equations. We first determine the branches of time-periodic solutions and examine the validity of our asymptotic analysis. We then investigate the transient behavior in the case of a subcritical Hopf bifurcation. In particular, we shall simulate numerically the annihilation experiments reported for many nerve-conduction problems where repetitive firing (i.e., stable electrical oscillations) may be turned on or off. As we shall demonstrate, our singular bifurcation analysis provides a clear understanding of this phenomenon. Finally, in § 5, we discuss the relation between our analysis and studies of bifurcations near double zero-eigenvalues [13]-[15].

2. Singular Hopf bifurcation.

2.1. Formulation. To obtain expansions of the time-periodic solutions that are valid near λ_0 as $\varepsilon \to 0$, we first propose an expansion of $\lambda - \lambda_0$ given by

$$\lambda - \lambda_0(0) = \varepsilon(l_1 + \varepsilon^{1/2} l_2 \cdots), \tag{2.1}$$

where the bifurcation point $\lambda_0(0)$ now satisfies the conditions

$$f_x(\lambda_0(0), 0) = 0, \tag{2.2}$$

$$-f_y(\lambda_0(0), 0) g_x(\lambda_0(0), 0) > 0 \tag{2.3}$$

which are obtained from (1.4) and (1.5) with $\varepsilon = 0$. Then, as suggested by (1.14), we seek asymptotic expansions of the solutions of (1.1) in the form

$$x(\tau, \varepsilon^{1/2}) - x_0(\lambda, \varepsilon) = \varepsilon^{1/2}(u_1(\tau) + \varepsilon^{1/2} u_2(\tau) \cdots), \tag{2.4}$$

$$y(\tau, \varepsilon^{1/2}) - y_0(\lambda, \varepsilon) = \varepsilon(v_1(\tau) + \varepsilon^{1/2} v_2(\tau) \cdots) \tag{2.5}$$

where τ is a new time variable suggested by (1.15) and defined by

$$\tau \equiv \varepsilon^{1/2} t. \tag{2.6}$$

The coefficients u_1, u_2, v_1, v_2 are determined by inserting (2.1), (2.4) and (2.5) into (1.1) and equating to zero the resulting coefficients of each power of $\varepsilon^{1/2}$. This leads to the following systems of equations for u_1, v_1 and u_2, v_2, respectively:

$$\begin{aligned} u_{1\tau} &= f_y v_1 + \tfrac{1}{2} f_{xx} u_1^2, \\ v_{1\tau} &= g_x u_1 \end{aligned} \tag{2.7}$$

and

$$\begin{aligned} u_{2\tau} - (f_y v_2 + f_{xx} u_1 u_2) &= (f_{x\lambda} l_1 + f_{x\varepsilon}) u_1 + f_{xy} u_1 v_1 + \tfrac{1}{6} f_{xxx} u_1^3, \\ v_{2\tau} - g_x u_2 &= g_y v_1 + \tfrac{1}{2} g_{xx} u_1^2 \end{aligned} \tag{2.8}$$

where f_x, f_{xx}, etc. represent partial derivatives evaluated at $x = x_0$, $y = y_0$, $\lambda = \lambda_0$ and $\varepsilon = 0$. The problems (2.7) and (2.8) can be simplified considerably if we introduce the new dependent and independent variables a, a_2, c, c_2 and s, defined by

$$a \equiv u_1/\alpha, \quad a_2 \equiv u_2/\alpha, \quad c \equiv v_1/\beta, \quad c_2 \equiv v_2/\beta, \quad s \equiv \sigma\tau, \tag{2.9}$$

where σ, α and β are given by

$$\sigma \equiv (-f_y g_x)^{1/2}, \quad \alpha \equiv \sigma/f_{xx}, \quad \beta \equiv -g_x/f_{xx}. \tag{2.10}$$

Introducing (2.9) into (2.7) and (2.8), we obtain

$$a_s = c + \tfrac{1}{2} a^2, \qquad c_s = -a \tag{2.11}$$

and

$$a_{2s} - (c_2 + a a_2) = La + Pac + Qa^3, \qquad c_{2s} + a_2 = Rc + Sa^2 \tag{2.12}$$

where the coefficients L, P, Q, R and S are defined by

$$L \equiv (f_{x\lambda} l_1 + f_{x\varepsilon})/\sigma, \quad P \equiv f_{xy}\beta/\sigma, \quad Q \equiv f_{xxx}\alpha^2/6\sigma, \quad R \equiv g_y/\sigma, \quad S \equiv \alpha^2 g_{xx}/2\sigma\beta. \tag{2.13}$$

Equations (2.7) and (2.8) or equivalently (2.11) and (2.12) are particularly useful for a phase-plane analysis. Recently, Eckhaus [16] analyzed the trajectories corresponding to (1.10). In particular, he considers the case where the nonlinearity is purely quadratic, i.e., he studies

$$x_t = y - x^2, \qquad y_t = -\varepsilon(x+\lambda) \tag{2.14}$$

and analyzes the perturbation produced by small $|\lambda|$. If $\lambda = 0$, (2.14) is equivalent to (2.11). Thus, we expect that the phase-plane analysis of (2.11) and (2.12) will be similar to the Eckhaus study of (2.14). The trajectories will be briefly analyzed in § 2.3 below.

On the other hand, if one is only interested in the periodic solutions of (2.11) and (2.12) and not in the transient behavior, it is more convenient to consider the equivalent systems of equations for a, $b \equiv -a_s$ and a_2, $b_2 \equiv -a_{2s}$, respectively. From (2.11) and (2.12) we find that these new variables satisfy

$$a_s = -b, \qquad b_s = a(1+b) \tag{2.15}$$

and

$$\begin{aligned} &a_{2s} = -b_2, \\ &b_{2s} - a_2(1+b) - ab_2 = (L+R)b - a^2\left(S - P - \frac{R}{2}\right) - Pb^2 + a^2 b\left(3Q - \frac{P}{2}\right). \end{aligned} \tag{2.16}$$

Equation (2.15) has been obtained as the leading order equation for an epidemic model [17]. It has a first integral given by

$$N \equiv a^2 + 2b - 2\ln|1+b|. \tag{2.17}$$

Using (2.17), the phase-plane analysis of (2.15) indicates that there exists a one-parameter family of periodic orbits surrounding the origin. The period of the oscillations is equal to 2π at the origin and progressively increases as the amplitude of the oscillations increases. Near the invariant line $b = -1$, the period becomes infinite. To obtain the explicit dependence of the amplitude of the oscillations on the bifurcation parameter, we must analyze the problem (2.16) for a_2 and b_2.

2.2. The periodic solutions. Since the homogeneous problem corresponding to (2.16) admits periodic solutions given by $a_2 = a_s$, $b_2 = b_s$, where $(a(s), b(s))$ represents a solution of (2.15) of period T_N ($2\pi \leqq T_N < \infty$), the right-hand side of (2.16) must satisfy a solvability condition. Using the solution of the adjoint homogeneous problem (see [17]), this condition requires that

$$\int_0^{T_N} ds \frac{b}{1+b}\left[b(L+R) - a^2\left(S - P - \frac{R}{2}\right) - Pb^2 + a^2 b\left(3Q - \frac{P}{2}\right)\right] = 0. \tag{2.18}$$

Note that $b(s)$ is even in s and

$$\int_0^{T_N} ds\, ba^2 = 0, \tag{2.19}$$

so that

$$\int_0^{T_N} ds \frac{b^2 a^2}{1+b} = \int_0^{T_N} ds \frac{b}{1+b}[a^2(1+b) - a^2] = -\int_0^{T_N} ds \frac{ba^2}{1+b}. \tag{2.20}$$

Thus the integral (2.18) reduces to the condition

$$\int_0^{T_N} ds \frac{b}{1+b}\left[b(L+R)-a^2\left(S-\frac{R}{2}+3Q-\frac{3P}{2}\right)-Pb^2\right]=0. \tag{2.21}$$

This equation represents the amplitude or bifurcation equation. It relates the amplitude of the oscillations corresponding to the period T_N to l_1 (appearing in L), the correction of the bifurcation parameter. In general, the integral must be computed numerically. However, it has two interesting limits corresponding to small and large amplitude oscillations.

A. Small amplitude solutions. For small values of N, the solution of (2.15) is given by

$$a(s', \nu)=\nu(e^{is'}+\text{c.c.})+\nu^2\left(-\frac{i}{3}e^{2is'}+\text{c.c.}\right)+O(\nu^3) \tag{2.22}$$

where

$$\nu \equiv \frac{1}{2\pi}\int_0^{2\pi} a(s', \nu)\, e^{-is'}\, ds'.$$

Thus, the maximum value of $a(s', \nu)$ corresponds to $2\nu+O(\nu^2)$. s' is a new time variable defined by

$$s' \equiv \omega(\nu)s=\left(1-\frac{\nu^2}{6}+O(\nu^4)\right)s. \tag{2.23}$$

Using the approximation (2.22) and the fact that $b=-\omega a_{s'}$, we find from (2.21) with $T_N=2\pi/\omega$ the following condition:

$$L+R+\nu^2\left(S-\frac{R}{2}+3Q-\frac{P}{2}\right)+O(\nu^4)=0. \tag{2.24}$$

Equation (2.24) provides a relation between the amplitude ν and the bifurcation parameter L. From the linear stability analysis of (x_0, y_0) we note that the basic state solution corresponding to $a=a_2=b=b_2=0$ is stable (or unstable) if

$$L+R<0 \qquad (L+R>0). \tag{2.25) (2.26}$$

Thus, condition (2.24) implies that the periodic solutions and a stable (unstable) steady state coexist under the same values of the parameters if the coefficient of ν^2 is positive (negative) i.e., if

$$\left(S-\frac{R}{2}+3Q-\frac{P}{2}\right)>0 \qquad (<0). \tag{2.27) (2.28}$$

The conditions (2.27), (2.28) describe the direction of bifurcation: the bifurcation is subcritical (supercritical) when (2.27) ((2.28)) is satisfied. As a consequence of the Hopf bifurcation theorem, [1], [2], the periodic solutions are unstable (stable) if (2.27) ((2.28)) is satisfied. We now examine the case of large amplitude solutions.

B. Large amplitude solutions. As $L+R$ progressively increases from zero, the amplitude of the periodic solution quickly increases and becomes infinite as L approaches a critical value $L=L_0$. The bifurcation diagram is given in Fig. 1. The critical point $L=L_0$ can be obtained from (2.21) with $N\to\infty$ using (2.17). In this limit, the periodic orbit spends most of its time near the line $b=-1$ and the period of the

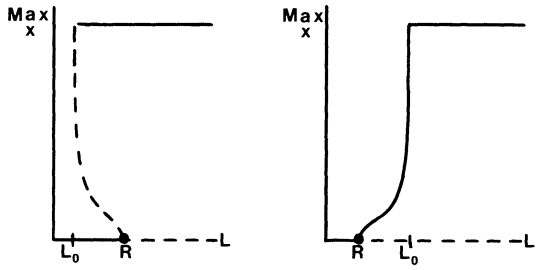

FIG. 1. *Bifurcation diagrams of the periodic solutions.* (a) *subcritical Hopf bifurcation,* (b) *supercritical Hopf bifurcation.*

oscillations approaches an infinite value. By evaluating asymptotically the integral (2.21), we find that $L = L_0$ satisfies the condition

$$L_0 + R + \left(S - \frac{R}{2} + 3Q - \frac{P}{2}\right) = 0. \tag{2.29}$$

Note by comparing (2.29) and (2.24) that $L_0 + R$ is a function of the direction of bifurcation defined by the conditions (2.27), (2.28).

2.3. Trajectories. In the preceding analysis, we have determined the bifurcation diagram of the small amplitude periodic solutions of (1.1). In order to investigate the general evolution of x and y in the vicinity of the basic solution, it is particularly instructive to examine the possible trajectories in the phase plane. By defining

$$A = (x - x_0)/\alpha\varepsilon^{1/2}, \quad C = (y - y_0)/\beta\varepsilon, \quad s = \varepsilon^{1/2}\sigma t, \tag{2.30}$$

where (x_0, y_0) corresponds to the basic steady-state solution and using (2.1), Equation (1.1) for x and y can be rewritten as

$$\begin{aligned} A_s &= C + \tfrac{1}{2}A^2 + \varepsilon^{1/2}(LA + PAC + QA^3) + O(\varepsilon), \\ C_s &= -A + \varepsilon^{1/2}(RC + SA^2) + O(\varepsilon) \end{aligned} \tag{2.31}$$

where the coefficients in (2.31) are defined in (2.9), (2.10) and (2.13). By comparing (2.31) and (2.11), (2.12), we conclude that $A = a + \varepsilon^{1/2}a_2 + O(\varepsilon)$ and $C = c + \varepsilon^{1/2}c_2 + O(\varepsilon)$. We now examine the possible trajectories $C = C(A, \varepsilon^{1/2})$ in the phase plane (C, A). As noticed by Eckhaus in his study of the "duck" trajectories [16], the long-time evolution of the system depends on its behavior near the separatrix curve defined by

$$C = C(A, \varepsilon^{1/2}) = -\tfrac{1}{2}A^2 + 1 + O(\varepsilon^{1/2}). \tag{2.32}$$

If $\varepsilon = 0$, (2.32) corresponds to the invariant line $b = -1$ since $b \equiv -a_s = -(c + \frac{1}{2}a^2)$. In the phase plane (b, a), the line $b = -1$ separates the region of the periodic orbits surrounding the origin $(b > -1)$ and trajectories leading to unbounded behaviors $(b < -1)$. Thus (2.32) also represents a separatrix curve between the periodic orbits and possible unbounded solutions. We investigate the behavior of the trajectories near (2.32) by seeking solutions of (2.31) of the form

$$C = C(A, \varepsilon^{1/2}) = -\tfrac{1}{2}A^2 + 1 + \varepsilon^{1/2}\theta(A) + O(\varepsilon). \tag{2.33}$$

Taking the ratio of the two equations (2.31) and introducing (2.33), we obtain the following equation for θ:

$$\frac{d\theta}{dA} - A\theta = R + \left(L + P + S - \frac{R}{2}\right)A^2 + \left(Q - \frac{P}{2}\right)A^4. \tag{2.34}$$

Equation (2.34) subject to the initial condition $\theta(A_0) = \theta_0$ admits the following solution:

$$\theta(A) = \theta_0\, e^{(A^2-A_0^2)/2} + e^{A^2/2} \int_{A_0}^{A} e^{-\xi^2} \left[R + \left(L + P + S - \frac{R}{2} \right) \xi^2 + \left(Q - \frac{P}{2} \right) \xi^4 \right] d\xi. \tag{2.35}$$

Assuming $A_0 < 0$ and $A > 0$, it is interesting to evaluate (2.35) asymptotically. Defining $\delta \equiv -A_0^{-1} \ll 1$ and assuming $A = \delta^{-1} z$, we find as $\delta \to 0$

$$\theta(z) \simeq \theta_0\, e^{\delta^{-2}(z^2-1)/2} + \sqrt{2\pi}\, e^{\delta^{-2} z^2/2} (L - L_0), \tag{2.36}$$

where L_0 is defined by (2.29). In order to keep the second term bounded, we assume that $L - L_0$ is an exponentially small quantity given by

$$L - L_0 = \mu\, e^{-\delta^{-2} k^2/2} \tag{2.37}$$

where $\mu = \pm 1$ if $L - L_0 \gtrless 0$ and k is an $O(1)$ constant. Then, if $k > 1$ (if $k < 1$) the first term (the second term) in (2.36) will be dominant when $z > 1$ ($z > k$). The possible cases are presented in Figs. 2 and 3. Except for cases 2a and 2b (i.e., supercritical Hopf bifurcation and $L < L_0$), the figures indicate that if A_0 is sufficiently negative, all trajectories leave the slow manifold at $A = K$. Such trajectories have been called "duck" trajectories and have been investigated in detail by Eckhaus [16] for the class of problems (1.10). For these equations, it is also possible to show that the duck trajectories are part of a large limit cycle solution (see the inset in Fig. 2).

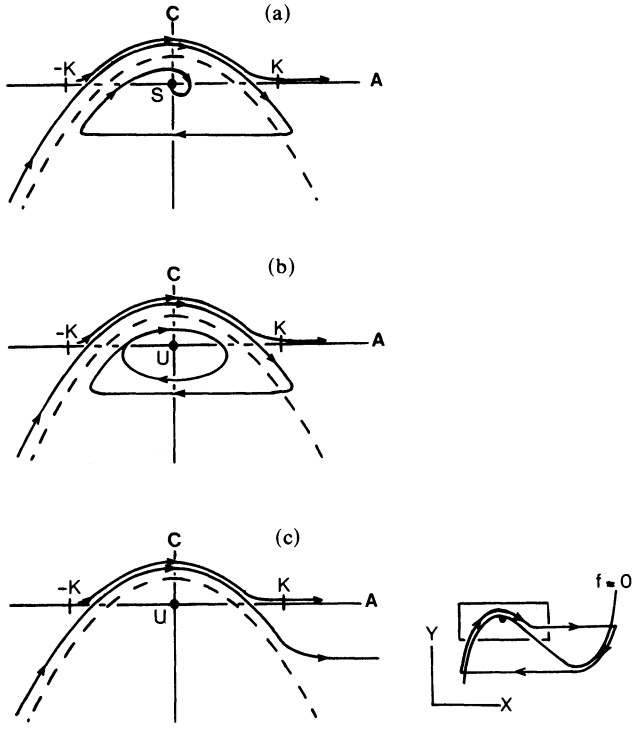

FIG. 2. *Trajectories in the phase plane* (A, C) *corresponding to the super critical Hopf bifurcation* (*Fig.* 1b). *The dashed curve is the separatrix of the periodic solutions and is defined by* (2.32). $K = \delta^{-1}k \gg 1$ *is related to* L *by* $L - L_0 = \mu \exp(-K^2/2)$. *In the figures,* S *and* U *denote a stable and an unstable singular point, respectively.* (a) $\mu = -1$ *and* $L < R$; (b) $\mu = -1$ *and* $R < L < L_0$; (c) $\mu = 1$ *or* $L > L_0$. *Note that in Fig.* 2b, *there exists a stable limit-cycle. In Fig.* 2c, *however, all trajectories are unbounded near the singular point but may be attracted by a large amplitude limit-cycle* (*see inset in Fig.* 2c).

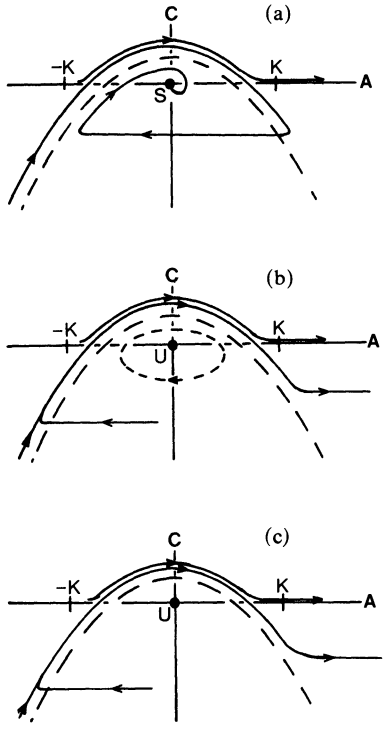

FIG. 3. *Trajectories in the phase plane* (A, C) *corresponding to the subcritical Hopf bifurcation* (*Fig.* 1a). *The dashed curve is defined by the parabola* (2.32). $K = \delta^{-1}k$ *is related to the bifurcation parameter* L *by* $L - L_0 = \mu \exp(-K^2/2)$. *S and U correspond to a stable and an unstable singular point, respectively.* (a) $\mu = -1$ *or* $L < L_0$; (b) $\mu = 1$ *and* $L_0 < L < R$; (c) $\mu = 1$ *and* $L > R$. *In Fig.* 3b *there exists an unstable limit-cycle surrounding a stable singular point.*

In summary, we have re-examined the Hopf bifurcation as ε tends to zero in (1.1). Our analysis which requires no additional assumptions on (1.1) indicates how the harmonically modulated, periodic solutions become progressively pulsating as the bifurcation parameter deviates from criticality. In addition, we have found a limit point where the amplitude of the oscillations become unbounded. Thus, our perturbation analysis becomes invalid in the vicinity of this point. Numerical studies of simple model equations indicate however that this quasi-vertical branch connects large-amplitude time-periodic solutions. They correspond to relaxation oscillations and may be described in the phase plane by a singular perturbation analysis [18]. In Fig. 1, we represent these solutions by a line parallel to the L-axis.

3. Chemical oscillations. The analysis of (1.1) was motivated by the fact that most chemical systems which exhibit oscillations experimentally can be modelled by two-variable equations of the form (1.1) with $\varepsilon \ll 1$. In this section, we illustrate our analysis by describing the transition to the time-periodic solutions of the Brusselator equations and the FitzHugh-Nagumo (FHN) equations. The Brusselator is a model chemical reaction suggested by Prigogine and Lefever [19] as perhaps the simplest oscillator obtainable from a chemical model based on the law of mass action. The FHN model is a modification of van der Pol's relaxation oscillator and is proposed to describe the electro-chemical activity in a nerve [1], [12]. Other applications of our analysis are possible. For example, the chemical reactor equations for a simple reaction $A \to B$

corresponds to two nonlinear equations for the temperature and the concentration [4]. The parameter ε appearing in these equations corresponds to the Lewis number. Another experimental example is provided by the Belousov-Zhabotinskii reaction. It is the best example of an oscillatory reaction and can also be described by two equations for two key intermediates [5], [6]. The parameter ε in (1.1) now corresponds to a ratio of kinetic constants and is an $O(10^{-2})$ quantity. Similarly, the glycolytic reaction which is the prototype of biochemical oscillations may also be studied by a two-variable model [8]. After appropriately rescaling the dependent and time variables, the model reduces to (1.1) with ε proportional to $L^{-1/2}$ where $L = O(10^6)$ is the allosteric constant of an allosteric enzyme.

From a practical point of view, our asymptotic analysis of (1.1) as $\varepsilon \to 0$ indicates how the relaxation oscillations appear from the Hopf bifurcation. It also leads to a simple determination of the limit point of a subcritical branch of periodic solutions. Moreover, the phase-plane analysis of (1.1) as $\varepsilon \to 0$ allows us to discuss the excitability properties of the stable steady state [5], [9], [20].

We first consider the Brusselator equations. The corresponding chemical model is the best example of an auto-catalytic reaction leading to chemical oscillations [21]. The kinetic equations for the concentration of the two chemical intermediates X and Y are given by

$$\begin{aligned} X_t &= A-(B+1)X+X^2Y, \\ Y_t &= BX-X^2Y \end{aligned} \tag{3.1}$$

where A and B correspond to two constant input products. Equations (3.1) admit a unique steady state

$$X_0 = A, \qquad Y_0 = \frac{B}{A} \tag{3.2}$$

which is unstable if

$$B > B_0 \equiv 1 + A^2. \tag{3.3}$$

We are interested in analyzing the special case $A \ll 1$. To this end, it is convenient to define the deviations from the steady state (3.2) by

$$x \equiv \frac{X-A}{A}, \qquad y \equiv \left(Y - \frac{B}{A}\right) A \tag{3.4}$$

and to rewrite the evolution equations (3.1) in terms of x and y:

$$\begin{aligned} x_t &= (B-1)x + By + B(x^2+2xy+x^2y), \\ y_t &= \varepsilon[-x-y-(x^2+2xy+x^2y)] \end{aligned} \tag{3.5}$$

where $\varepsilon \equiv A^2 \ll 1$. We now apply our theory. We seek a solution of (3.5) of the form (2.1), (2.4) and (2.5) where $\lambda = B$, $\lambda_0 = 1$, $x_0 = 0$ and $y_0 = 0$. We then obtain from (2.10) and (2.13) that $\sigma = 1$, $\alpha = \beta = \frac{1}{2}$, $L = l_1$, $P = 1$, $Q = 0$, $R = -1$ and $S = -\frac{1}{2}$. Introducing these values into (2.24), we find that the amplitude ν of the small amplitude periodic solutions is given by

$$\nu = \sqrt{2(l_1 - 1)} + O(l_1 - 1). \tag{3.6}$$

Thus the bifurcation is always supercritical ($l_1 > 1$ corresponds to $B > 1 + A^2$ and therefore to unstable steady states). From (2.29), we then obtain the limit point of the large amplitude periodic solutions

$$l_1 = L_0 = \tfrac{3}{2}. \tag{3.7}$$

The bifurcation diagram of the periodic solution of the Brusselator as $A \to 0$ corresponds to Fig. 1b.

We now apply the results of our analysis to the FHN equations. The properties of its solutions have been extensively studied because it is believed to model many aspects of nerve conduction [11], [12]. In addition, the solutions of other more complicated nerve conduction problems such as the Hodgkin-Huxley equations [22] may share similar properties with those of the FHN equations. The FHN equations for the space-clamped nerve are given by

$$\begin{aligned} v_t &= -F(v) - w + I, \\ w_t &= \varepsilon(v - \gamma w) \end{aligned} \tag{3.8}$$

where $F(v) = v(v-1)(v-a)$ and $0 < a < \frac{1}{2}$. The variables v and w correspond to the membrane potential and a slowly-varying recovery variable. I is the constant input current and represent the control parameter. The other parameters a, γ and ε are fixed quantities. If

$$\gamma < \gamma_c \equiv 3/(a^2+1-a), \tag{3.9}$$

equations (3.8) admit only one steady-state solution $v = \bar{v}$ and $w = \bar{v}/\gamma$ where $\bar{v}$ satisfies

$$I = F(\bar{v}) + \frac{\bar{v}}{\gamma}. \tag{3.10}$$

It is mathematically more convenient to consider $\bar{v} = \bar{v}(I)$ as the control parameter and to rewrite the evolution equations (3.8) in terms of the deviations $x = v - \bar{v}$ and $y = w - \bar{v}/\gamma$. We then find from (3.8) that x and y satisfy

$$\begin{aligned} x_t &= -F'(\bar{v})x - y - F''(\bar{v})\frac{x^2}{2} - x^3, \\ y_t &= \varepsilon(x - \gamma y). \end{aligned} \tag{3.11}$$

We now follow the asymptotic analysis proposed in § 2. First we define the Hopf bifurcation point $\bar{v} = v^*$ as one of the two solutions of

$$F'(\bar{v}) \equiv 3v^{*2} - 2v^*(a+1) + a = 0. \tag{3.12}$$

Then we expand the bifurcation parameter as

$$\bar{v}(\varepsilon) - v^* = \varepsilon(l_1 + \varepsilon^{1/2} l_2 \cdots) \tag{3.13}$$

and seek a solution of (3.11) of the form (2.4), (2.5) with $x_0 = y_0 = 0$. From (2.10) and (2.13), we find that

$$\begin{aligned} &\sigma = 1, \quad \alpha = -\frac{1}{F''(v^*)}, \quad \beta = \frac{1}{F''(v^*)}, \\ &L = -F''(v^*)l_1, \quad P = S = 0, \quad Q = -\frac{1}{F''(v^*)^2}, \quad R = -\gamma. \end{aligned} \tag{3.14}$$

As a consequence, the amplitude equations (2.24) and (2.29) give the following results for ν and L_0:

$$\nu = \sqrt{2(L-\gamma)/(\gamma_0 - \gamma)} + O(L-\gamma) \tag{3.15}$$

and

$$L_0 = \gamma + \tfrac{1}{2}(\gamma_0 - \gamma), \tag{3.16}$$

where

$$\gamma_0 \equiv \frac{6}{F''(v^*)^2}.$$

We conclude from (3.15) that the bifurcation is supercritical (subcritical) if $L > \gamma$ and $\gamma < \gamma_0$ ($L < \gamma$ and $\gamma > \gamma_0$). Moreover the periodic solutions admit a limit point given by (3.16). The bifurcation diagrams are given in Figs. 1a and 1b for the cases $\gamma > \gamma_0$ and $\gamma < \gamma_0$ respectively. Note that although the basic steady state is stable if $L < \gamma$, small perturbations of the steady state may lead to an unbounded behavior. These "excitability" properties of the steady state can be well understood by the phase-plane analysis of § 2.3 (see Fig. 2a).

4. Numerical results. In this section, we investigate numerically the FHN equations and discuss the validity of our asymptotic analysis. We first determine the bifurcation diagram of the periodic solutions. We use a computer program which finds steady and periodic solution branches using continuation methods and determines their stability properties [25]. We then consider the case of a subcritical bifurcation and analyze how the FHN system may reversibly switch between two stable regimes, in response to a small perturbation. By means of phase planes, we show that the timing of this perturbation is particularly important and may be predicted by our singular bifurcation analysis.

4.1. Bifurcation diagrams. The results of our analysis of the FHN equations (3.8) indicate that bifurcation is either supercritical or subcritical ($\gamma < \gamma_0$ or $\gamma > \gamma_0$). Consequently, the two bifurcation diagrams sketched in Figs. 1a and 1b are possible diagrams for the FHN model. They are given in Figs. 4 and 5. In these figures, we represent the maximum value of v as a function of the applied current I (curve (iii)). The curves (i) and (ii) correspond to two different approximations proposed by our asymptotic analysis of the FHN equations. We now describe these results in detail. In §§ 2 and 3, we found that the periodic solutions are given by

$$\begin{aligned} v - \bar{v} &= -\varepsilon^{1/2} a / F''(v^*) + O(\varepsilon), \\ w - \bar{v}/\gamma &= \varepsilon c / F''(v^*) + O(\varepsilon^{3/2}), \end{aligned} \tag{4.1}$$

where $\bar{v}(I)$ corresponds to the steady state and is defined by (3.10). The two variables a and c are periodic functions of $s = \varepsilon^{1/2} t$ and satisfy (2.11). These periodic solutions are analyzed in § 2 by studying the equivalent system of equations for a and $b = -a_s$. It has a first integral given by (2.17) where N is an integration constant ($0 \leqq N < \infty$). By using (2.17) and analyzing the periodic solution in the phase plane (a, b), we note that the maximum amplitude for a corresponds to $b = 0$ and is given by

$$a_M = N^{1/2}. \tag{4.2}$$

This information will be useful for determining the bifurcation diagram of the periodic solutions. To obtain N as a function of the control parameter I, we must solve the solvability condition (2.21). This condition for the FHN model may be reformulated as

$$\int_0^{T_N} ds \frac{b}{1+b} \left[b(L-\gamma) + \frac{a^2}{2}(\gamma - \gamma_0) \right] = 0, \tag{4.3}$$

where T_N is the period of the oscillations corresponding to $a = a(N, s)$ and $b = b(N, s)$, and γ_0 is defined by (3.16). L is related to the control parameter I: from (3.13) and using the steady-state relation (3.10), we have

$$I - I^* = -\frac{\varepsilon L}{F''(v^*)} + O(\varepsilon^{3/2}) \tag{4.4}$$

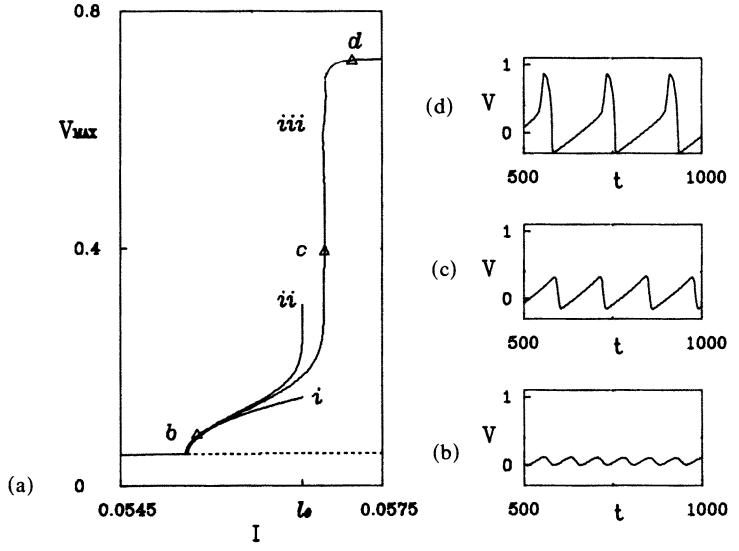

FIG. 4. (a) *Comparison between the numerical branch of solutions and the asymptotic branch of solutions for a supercritical Hopf bifurcation of the FHN equations. The values of the parameters are* $\varepsilon = 0.008$, $\gamma = 1$ *and* $a = 0.1$. *Solid and dashed curves represent stable and unstable solutions, respectively.* (i) *is an asymptotic approximation for small values of N, curve* (ii) *is an asymptotic approximation for all values of N and is obtained when* (4.6) *is computed numerically and curve* (iii) *is the numerical branch of solutions. The limit point is* $l_0 = 0.05678$. *The points* b, c *and* d *in Fig.* 4a *correspond to the periodic solutions given in Figs.* 4b, c *and* d. *They indicate the transition from small harmonic oscillations to large amplitude, relaxation oscillations. The values of the control parameter I corresponding to Figs.* 4b, c *and* d *are* $I = 0.05527$, 0.05683 *and* 0.05740, *respectively.*

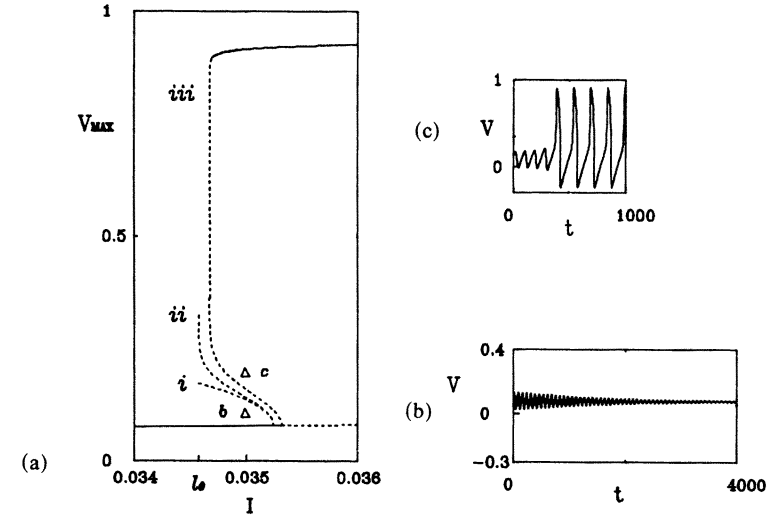

FIG. 5. *Comparison between the numerical branch of solutions and the asymptotic branch of solutions for a subcritical Hopf bifurcation of the FHN equations. The values of the parameters are* $\varepsilon = 0.008$, $\gamma = 2.54$ *and* $a = 0.14$. *Solid and dashed curves represent stable and unstable solutions, respectively. Curve* (i) *is an asymptotic approximation for small values of N, curve* (ii) *is an asymptotic approximation for all values of N when* (4.6) *is computed numerically and curve* (iii) *is the numerical branch of solutions. The limit point is* $l_0 = 0.03457$. *The points* b *and* c *in Fig.* 5a *correspond to the initial voltage perturbations from the steady state when* $I = 0.035$. *They are given by:* $v(0) = 0.1200$, $w(0) = 0.03053$ (*point* b) *and* $v(0) = 0.1285$, $w(0) = 0.03053$ (*point* c). *The trajectories emerging from these initial conditions are shown in Figs.* 5b *and* 5c.

where I^* is defined by (3.10) with $\bar{v} = v^*$. To determine $L = L(N)$ or $I = I(N)$, we fix the value of N and find $a(N, s)$ and $b(N, s)$ by integrating numerically Equation (2.11), with $a(N, O) = a_M$ and $b(N, O) = 0$. We then evaluate integral (4.3) and determine $L(N)$. Curve (ii) in Figs. 4 and 5 gives the approximate maximum value of v defined by

$$v_M = v^* - \frac{\varepsilon^{1/2} a_M}{F''(v^*)} \tag{4.5}$$

as a function of $I(N)$ given by (4.4) with $L(N)$. Both in the supercritical case (Fig. 4) and in the subcritical case (Fig. 5), the branch of periodic solutions admits a limit point, denoted by l_0, which corresponds to $L = L_0$ given by (3.16). We note that the approximate branch of solutions (ii) deviates from the numerical branch of solutions by $O(10^{-3})$ quantities. They correspond to the order of magnitude of the correction terms neglected in our approximation. Thus, we conclude that there is a good quantitative agreement between the perturbation analysis and the numerical results. Curve (i) represents an approximation of integral (4.3) valid for small N. It is described by (2.22)-(2.24) and corresponds to small amplitude periodic solutions. This limit has been analyzed for the FHN equations and is given by (3.15). As expected, this approximation is only useful near the Hopf bifurcation point. From a qualitative point of view, our asymptotic analysis indicates how the harmonic oscillations (Fig. 4b) progressively change to become saw-toothed near the limit point (Fig. 4c). Thus, these pulsed, triangular oscillations represent an intermediate regime between the harmonic oscillations (Fig. 4b) and the relaxation oscillations (Fig. 4d) appearing at larger amplitudes.

We now consider the subcritical case (Fig. 5) in detail and analyze the transient behavior. Specifically, we study the response of the system due to two distinct and small perturbations of the stable steady state at $I = 0.035$. Points (b) and (c) in Fig. 5a correspond to the initial conditions $w = \bar{v}/\gamma$ and $v = \bar{v} + u$ where $(v, w) = (\bar{v}, \bar{v}/\gamma)$ is the steady state and u is the perturbation. Figures 5b and 5c give the response of the FHN system. The initial condition (b) leads to a slow decline to the stable steady state (Fig. 5b). The initial condition (c) leads to large amplitude relaxation oscillations after an induction period where the oscillations remain small (Fig. 5c). This bistability phenomenon can be better understood if we analyze the trajectories in the (v, w) phase plane. See Fig. 6. In this figure, we represent the unstable limit cycle surrounding the stable singular point as a dashed curve. This closed orbit separates in the phase plane the initial points leading to a stable focus from those leading to a stable limit cycle. Note that parabola (2.32) is a good approximation of the unstable periodic solution in the vicinity of the singular point. This parabola was previously analyzed as the separatrix curve of the periodic solutions. In terms of the variables v and w, this parabola is in first approximation given by

$$w - \frac{\bar{v}}{\gamma} \simeq -\frac{F''(v^*)(v - \bar{v})^2}{2} + \frac{\varepsilon}{F''(v^*)}. \tag{4.6}$$

A detailed analysis of the trajectories in the phase plane show that there exist three types of responses for the FHN model: (1) a perturbation of the stable steady-state interior to the unstable orbit spirals toward the steady state; (2) a perturbation exterior to the unstable limit cycle but above the parabola (4.6) spirals outward to the large amplitude and stable limit-cycle; (3) a perturbation exterior to the unstable limit cycle and below the parabola (4.6) leads directly to the stable limit cycle, without oscillating first near the unstable periodic solution. These observations are in agreement with our

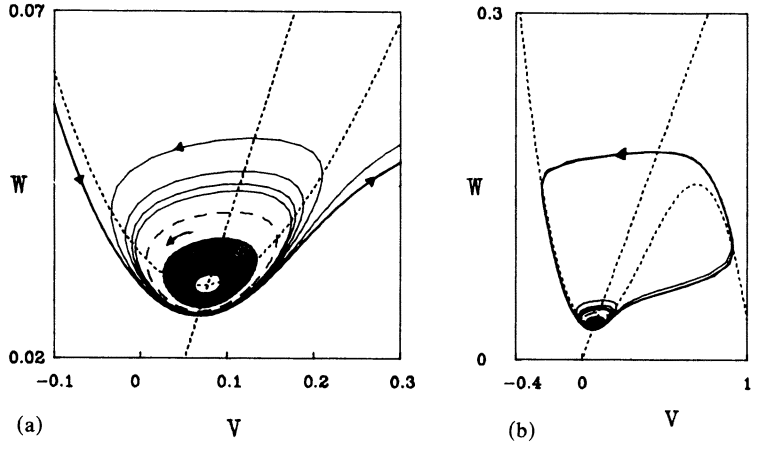

FIG. 6. *Phase plane portraits associated with the solutions shown in Figs.* 5b *and* 5c. *The small amplitude decaying oscillations in Fig.* 5b *correspond to the dense spiral in Fig.* 6a. *This spiral is approaching the stable singular point defined as the intersection of the v and w nullclines. (They are represented in the figure by broken lines.) Any perturbation within the unstable limit-cycle (dashed closed curve), spirals toward the stable steady state. In Fig.* 6b, *we show a trajectory which starts outside the unstable limit-cycle, oscillates four times in the vicinity of the unstable orbit and then exits to the large amplitude limit-cycle.*

previous analysis of the trajectories given in § 2. Thus, we conclude that the long-time behavior of the FHN system is particularly sensitive to small changes in the initial conditions near the singular point and the separatrix curve defined by (4.6). The physical significance of these results is discussed in the next subsection.

4.2. Annihilation experiments. Switching from a stable steady state to a stable periodic solution, or the reverse transition, can occur if the FHN system is operating near the stable singular point. Here, an appropriate, small perturbation is sufficient to induce the switching process. The unstable periodic solution, or its parabolic approximation (4.6) near the singular point, acts as a separatrix between the two stable regimes. This particular sensitivity to external perturbations and the importance of their timing has been observed in several nerve conduction problems [32], [33]. Guttman et al. [26], for example, have shown experimentally that repetitive firing in space-clamped squid axons can be annihilated by a brief pulse of current if the pulse is applied with the proper magnitude and at the proper time. Annihilation was also observed by Teorell [27] in a two-variable model of a sensory pacemaker neuron and by Best [28] using the Hodgkin–Huxley equations. These observations can be related to Winfree's work [29] on the suppression of rhythmic activity by critical perturbations. More complex situations involving two stable periodic solutions have also been investigated by Moran and Goldbeter [30].

We now analyze the annihilation experiments by integrating the FHN equations numerically. We present in Figs. 7–9 the results of our investigation. In these figures, we give both the response $v = v(t)$ and the corresponding trajectory in the (v, w) phase plane. We consider the same parameter values as in Fig. 6. That is, they correspond to the case of a stable limit cycle enclosing an unstable limit cycle and a stable singular point. In each experiment, we assume that the system is undergoing repetitive firing i.e., it produces stable relaxation oscillations. At a specific time $t = t_p$, a small step current i ($I = 0.035 + i$) is quickly turned on and off. Proper timing of this impulse and

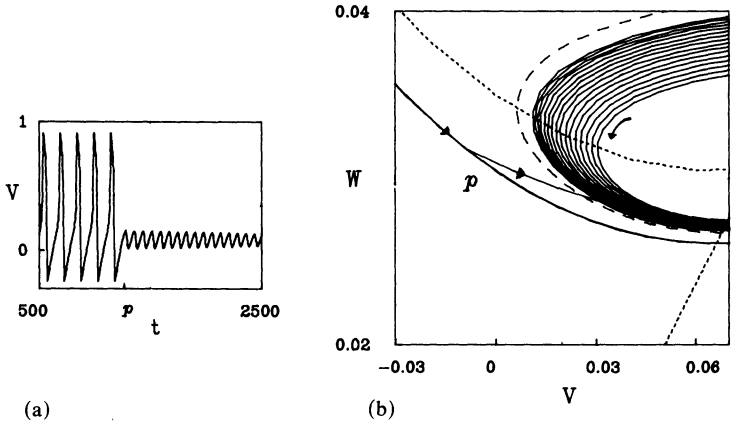

FIG. 7. *Stable large amplitude oscillations are annihilated by a small depolarizing perturbation. In* (a), *annihilation occurs when the applied current is changed from* $I = 0.035$ *to* $I = 0.038$ *at* $t = p$ *during a small interval of time. In* (b), *we present the phase plane portrait of this annihilation. When the perturbation is introduced at* $t = p$, *the trajectory is shifted to the unstable limit-cycle, crosses it and then spirals toward the stable singular point.*

the appropriate pulse intensity are two crucial factors for annihilation to occur. In Figs. 7 and 8, we observe the effect of a depolarizing perturbation ($i > 0$) and a hyperpolarizing perturbation ($i < 0$), respectively. In both cases, the perturbation is sufficient to induce a switch from stable oscillations to a stable steady state. As shown by the phase-plane analysis, the transition is only successful if the perturbation is applied at an appropriate phase. The importance of a threshold for these perturbations is illustrated in Fig. 9. In this figure, the perturbation is not strong enough to shift the

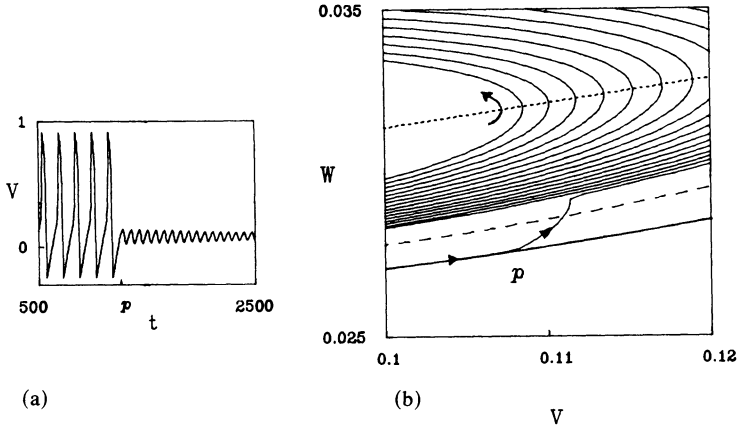

FIG. 8. *Stable large amplitude oscillations are annihilated by a small hyperpolarizing perturbation. In* (a), *annihilation occurs when the applied current is changed from* $I = 0.035$ *to* $I = 0.032$ *at* $t = p$ *during a small interval of time. In* (b), *we present the phase plane portrait corresponding to this experiment. When the perturbation is introduced at* $t = p$, *the trajectory is shifted to the unstable limit-cycle and then spirals toward the stable steady state.*

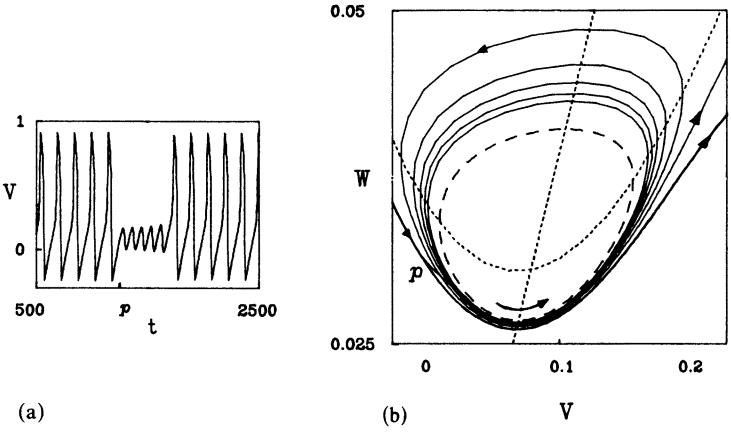

FIG. 9. *Stable large amplitude oscillations are perturbed into subthreshold oscillations. In* (a), *large amplitude oscillations are temporarily annihilated by changing the applied current from* $I = 0.035$ *to* $I = 0.037$ *at* $t = p$ *and then returning it to* $I = 0.035$ *at* $t = p + 6$. *In* (b), *the phase plane portrait of this failed annihilation experiment is shown. When the perturbation is introduced at* $t = p$, *the trajectory oscillates five times around the unstable orbit before returning to the large amplitude oscillations.*

trajectory to the inner region of the unstable limit cycle. Consequently, the system produces a few subthreshold oscillations around the unstable orbit and then returns to the stable limit cycle (see Fig. 9b).

These annihilation experiments are most successful when the critical phase range is large. We observe numerically that this range is largest for values of I approaching the limit point of the two limit cycles. In § 2, we have shown that when the control parameter approaches the limit point, a large part of the unstable limit cycle and a large part of the stable limit cycle are close to the slow-manifold curve defined by parabola (4.6). Consequently, a large part of the separatrix curve is in the vicinity of the stable limit cycle. If the stable limit cycle is slightly perturbed in this region, the system will be attracted by the stable singular point.

5. Discussion. We have analyzed the Hopf bifurcation of (1.1) as ε approaches zero. By contrast to classical Hopf bifurcation studies we show that the small-amplitude periodic solutions which appear at the bifurcation point as harmonic oscillations progressively become pulsating. The oscillations then represent a repetition of triangular pulses. As the bifurcation parameter approaches a critical limit point, the amplitude of these pulses and their period tend to infinity. We also show that the transient behavior in the vicinity of the steady or time-periodic solutions critically depends on the initial condition. Indeed, we determine in the phase plane, a separatrix curve which separates bounded and unbounded trajectories. These unbounded trajectories may be part of a large limit cycle which is not described by our analysis.

Our analysis is essentially a perturbation of a double zero eigenvalue appearing when $\varepsilon = 0$ and $\lambda = \lambda_0(0)$. Our study of the two variables equations (1.1) can be extended to a larger system of equations of the form

$$\begin{aligned} \mathbf{x}_t &= \mathbf{f}(\mathbf{x}, y, \gamma, \varepsilon), \\ y_t &= \varepsilon g(\mathbf{x}, y, \gamma, \varepsilon) \end{aligned} \tag{5.1}$$

where $\mathbf{x} = \text{col}\,(x_1, x_2 \cdots x_n)$ and $\mathbf{f}$ are n-dimensional vectors. Provided that the linearized problem

$$\begin{aligned} \mathbf{u}_t &= \mathbf{f}_{\mathbf{x}}(\mathbf{x}_0, y_0, \lambda_0, 0)\mathbf{u} + \mathbf{f}_y(\mathbf{x}_0, y_0, \lambda_0, 0)v, \\ v_t &= 0 \end{aligned} \tag{5.2}$$

admits a double zero eigenvalue and that $\mathbf{u}_t = \mathbf{f}_x(\mathbf{x}_0, y_0, \lambda_0, 0)\ \mathbf{u}$ has a simple zero eigenvalue, we found the same results as in § 2. The coefficients appearing in the amplitude equations are now determined by inner products of the derivatives of $\mathbf{f}$ and g with the critical mode. We emphasize that this double zero eigenvalue problem does not result from the coalescence of a Hopf bifurcation point and a steady bifurcation or limit point. Rather, it corresponds to a bifurcation to periodic solutions at low frequency. In this context, a particular example has been analyzed by Davis and Rosenblat [23]. Although they study the singular bifurcation in detail, their analysis leads to different amplitude equations and different conclusions. This difference results from the fact that the linearized problem in their case is given by

$$\begin{pmatrix} u_t \\ v_t \end{pmatrix} \equiv M \begin{pmatrix} u \\ v \end{pmatrix} \tag{5.3}$$

where the matrix M is defined by

$$M \equiv \begin{pmatrix} 0 & 0 \\ 0 & 0 \end{pmatrix}, \tag{5.4}$$

while in our case, M is given by

$$M \equiv \begin{pmatrix} 0 & 1 \\ 0 & 0 \end{pmatrix}. \tag{5.5}$$

The results of our analysis also differs from double zero eigenvalue problems which result from the coalescence of a steady and a Hopf bifurcation points even if they admit the same basic linearized matrix (5.5).

In the second part of the paper (§§ 3 and 4), we considered two applications of our theory. We first analyzed the Brusselator because it is the simplest model describing chemical oscillations. We then studied the FHN equations which are a prototype model for nerve conduction problems. The FHN model depends on two more parameters than the Brusselator and the bifurcation possibilities are more important. The case of $\varepsilon \to 0$ is not the only singular limit. Other singular limits or combinations of singular limits may lead to similar results (for example the case $a = O(\varepsilon)$). A detailed discussion of other interesting singular cases will be presented elsewhere. In § 4, the FHN equations were analyzed numerically. We have shown that the structure of the bifurcation diagrams as $\varepsilon \to 0$ can be determined analytically. Furthermore, motivated by the analysis of the trajectories in the phase plane, we investigated the complex response of the FHN model when a stable periodic solution coexists with a stable steady state. We then associated the results of this analysis with the annihilation experiments reported in he nerve conduction literature. Since a subcritical Hopf bifurcation is a prominent feature of several nerve conduction problems (see for example the numerical study of the Hodgkin-Huxley equations by Rinzel and Miller [31]), we expect that similar responses may be observed for more complicated models. Other interesting dynamical responses of the FHN equations may be possible near the singular Hopf

bifurcation point. In the near future, we shall explore the excitability properties of a unique stable steady state or a stable periodic solution.

REFERENCES

[1] L. N. HOWARD, *Nonlinear oscillations*, in Nonlinear Oscillations in Biology, Lectures in Applied Mathematics 17, American Mathematical Society, Providence, RI, 1979.

[2] The translation of the E. Hopf paper can be found in J. E. Marsden and M. McCracken, *The Hopf Bifurcation and Its Applications*, Applied Mathematical Sciences 19, Springer-Verlag, New York, 1976.

[3] B. VAN DER POL, *On relaxation-oscillations*, Phil. Mag., 7th Ser., 2 (1926), pp. 978-992.

[4] W. H. RAY AND S. P. HASTINGS, *The influence on the Lewis number on the dynamics of chemically reacting systems*, Chem. Eng. Sci., 35 (1980), pp. 589-595.

[5] J. J. TYSON, *Analytic representation of oscillations, excitability and traveling waves in a realistic model of the Belousov-Zhabotinskii reaction*, J. Chem. Phys., 66 (1977), pp. 905-915.

[6] ———, *Relaxation oscillations in the revised Oregonator*, J. Chem. Phys., 80 (1984), pp. 6079-6082.

[7] A. GOLDBETER AND S. R. CAPLAN, *Oscillatory enzymes*, Ann. Rev. Biophys. Bioengng., 5 (1976), pp. 449-476.

[8] A. GOLDBETER AND G. NICOLIS, *An allosteric enzyme model with positive feedback applied to glycolytic oscillations*, Prog. Theor. Biol., 4 (1976), pp. 65-157.

[9] H.-S. HAHN, A. NITZAN, P. ORTOLEVA AND J. ROSS, *Threshold excitations, relaxation oscillations, and effect of noise in an enzyme reaction*, Proc. Nat. Acad. Sci. USA, 71 (1974), pp. 4067-4071.

[10] I. R. EPSTEIN, K. KUSTIN, P. DE KEPPER AND M. ORBAN, *Oscillating chemical reactions*, Scientific American (March 1983), pp. 112-123.

[11] R. FITZHUGH, *Impurities and physiological states in theoretical models of nerve membrane*, Biophys. J., 1 (1961), pp. 445-466.

[12] J. RINZEL AND J. P. KEENER, *Hopf bifurcation to repetitive activity in nerve*, this Journal, 43 (1983), pp. 907-922.

[13] N. KOPELL AND L. N. HOWARD, *Bifurcations and trajectories joining critial points*, Adv. in Math., 18 (1975), pp. 306-358.

[14] J. P. KEENER, *Infinite period bifurcation and global bifurcation branches*, this Journal, 41 (1981), pp. 127-144.

[15] J. F. MAGNAN AND E. L. REISS, *Double-diffusive convection and λ-bifurcation*, Phys. Rev. A, 31 (1985), pp. 1841-1854.

[16] W. ECKHAUS, *Relaxation oscillations including a standard chase on french ducks*, Lecture Notes in Mathematics 985, Springer-Verlag, Berlin, 1983, pp. 432-449.

[17] I. B. SCHWARTZ AND H. L. SMITH, *Infinite subharmonic bifurcation in an* SEIR *epidemic model*, J. Math. Biol., 18 (1983), pp. 233-253.

[18] J. KEVORKIAN AND J. D. COLE, *Perturbation Methods in Applied Mathematics*, Applied Mathematical Sciences 34, Springer-Verlag, Berlin 1981.

[19] I. PRIGOGINE AND R. LEFEVER, *Symmetry breaking instabilities in dissipative systems*, II, J. Chem. Phys., 48 (1968), pp. 1695-1700.

[20] A. GOLDBETER, T. ERNEUX AND L. A. SEGEL, *Excitability in the adenylate cyclase reaction in Dictyostelium discoideum*, FEBS Lett., 89 (1978), pp. 237-241.

[21] G. NICOLIS AND I. PRIGOGINE, *Self-Organization in Nonequilibrium Systems*, John Wiley, New York, 1977.

[22] J. RINZEL, *Integration and propagation of neuro electric signals*, in Studies in Mathematical Biology, Part I, MAA Studies in Mathematics, 15, 1978, pp. 1-66.

[23] S. H. DAVIS AND S. ROSENBLAT, *On bifurcating periodic solutions at low frequency*, Stud. Appl. Math., 57 (1977), pp. 59-76.

[24] R. J. FIELD AND M. BURGER, *Oscillations and Traveling Waves in Chemical Systems*, Wiley-Interscience, New York, 1985.

[25] E. J. DOEDEL, AUTO, *A program for the automatic bifurcation analysis of autonomous systems*, Congressus Numerantium, 30 (1981), pp. 265-284.

[26] R. GUTTMAN, S. LEWIS AND J. RINZEL, *Control of repetitive firing in squid axon membrane as a model for a neuroneoscillator*, J. Physiol., 305 (1980), pp. 377-395.

[27] T. TEORELL, *A biophysical analysis of mechano-electrical transduction*, in Handbook of Sensory Physiology, I. Principles of Receptor Physiology, W. R. Loewenstein, ed., Springer-Verlag, Berlin, 1971.

[28] E. N. BEST, *Null space in the Hodgkin-Huxley equations. A critical test*, Biophys. J., 27 (1979), pp. 87-104.
[29] A. T. WINFREE, *The Geometry of Biological Time*, Springer-Verlag, Berlin, 1980.
[30] F. MORAN AND A. GOLDBETER, *Onset of birhythmicity in a regulated biochemical system*, Biophys. Chem., 20 (1984), pp. 149-156.
[31] J. RINZEL AND R. N. MILLER, *Numerical calculation of stable and unstable periodic solutions to the Hodgkin-Huxley equations*, Math. Biosc., 49 (1980), pp. 27-59.
[32] T. R. CHAY AND Y. S. LEE, *Impulse responses of automaticity in the Purkinje fiber*, Biophys. J, 45 (1984), pp. 841-849.
[33] ———, *Phase resetting and bifurcation in the ventricular myocardium*, Biophys. J., 47 (1985), pp. 641-651.